Acta Cryst E CRYSTALLOGRAPHIC COMMUNICATIONS

ISSN 2056-9890

Crystal structure and Hirshfeld surface analysis of dichlorido{2,2′-[oxybis(methylidene)]dipyridine}-mercury(II)

Jesse J. Derringer and Deborah C. Bebout*

Department of Chemistry, William & Mary, Williamsburg, VA 23187-8795, USA. *Correspondence e-mail: dcbebo@wm.edu

Received 30 September 2022
Accepted 12 November 2022

Edited by C. Schulzke, Universität Greifswald, Germany

Keywords: crystal structure; mercury complex; Hirshfeld surface analysis.

CCDC reference: 2219283

Supporting information: this article has supporting information at journals.iucr.org/e

The series of divalent metal chloride complexes of 2,2′-[oxybis(methylidene)]dipyridine (**L**) was extended with the preparation of the title compound, $[HgCl_2(C_{12}H_{12}N_2O)]$ or $[Hg\mathbf{L}Cl_2]$ (**1**). The Hg^{2+} complex crystallizes in $P2_1/n$, isomorphic with dichloride Co^{2+}, Cu^{2+}, Zn^{2+} and Cd^{2+} complexes of **L**. Metal ions of the isotypic complexes are coordinated by two chlorine atoms, as well as the oxygen atom and both nitrogen atoms of **L**. The complexes have a square-pyramidal coordination geometry with a chlorine atom in the apical position. Supramolecular interactions in **1** include offset face-to-face interactions between inversion-related complexes, leading to the formation of sheets parallel to the *ab* plane. Weak intermolecular H···Cl contacts link the sheets. Hirshfeld surface analysis indicates that H···H (36.5%), Cl···H/H···Cl (36.5%) and C···H/H···C (11.6%) interactions are dominant.

1. Chemical context

Structural comparisons of group 12 metal ions in similar environments can help improve understanding of the effects of metal-ion replacement on the biological properties of organic molecules. Ether-containing bioactive compounds with group 12 metal ion-dependent bioactivity include flavonoids (Sreenivasulu *et al.*, 2010; Kim *et al.*, 2011; Li *et al.*, 2017), ionophores (Ivanova *et al.*, 2011), and pharmaceuticals (Zhang *et al.*, 2014). Recent studies of 2,2′-[oxybis(methylidene)]dipyridine (**L**) with group 12 perchlorate salts revealed bis-tridentate chelate $[M\mathbf{L}_2](ClO_4)_2$ complexes with either meridional octahedral (M = Zn^{2+} or Cd^{2+}) or trigonal–prismatic (M = Hg^{2+}) metal-ion coordination (Sturner *et al.*, 2022). Isotypic square-pyramidal $[M\mathbf{L}Cl_2]$ complexes of Zn^{2+} (τ = 0.03) and Cd^{2+} (τ = 0.11) have been reported previously (Addison *et al.*, 1984; Li, 2008*a*,*b*). Herein, the preparation, crystal structure and Hirshfeld surface analysis of dichlorido{2,2′-[oxybis(methylidene)]dipyridine}mercury(II) is reported.

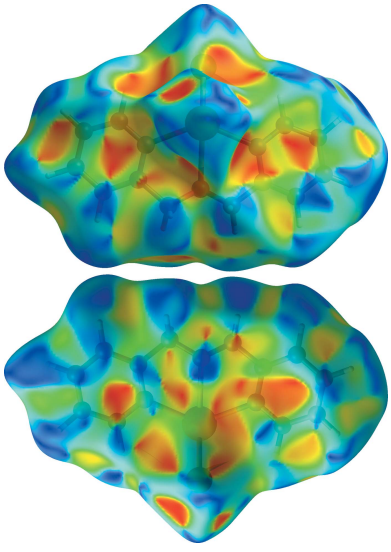

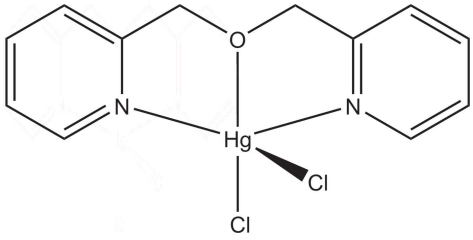

Table 1
Selected geometric parameters (Å, °).

Hg1—N2	2.323 (2)	Hg1—Cl2	2.4598 (7)
Hg1—N1	2.324 (2)	Hg1—O1	2.5831 (18)
Hg1—Cl1	2.4515 (6)		
N2—Hg1—N1	129.28 (8)	Cl1—Hg1—Cl2	120.18 (2)
N2—Hg1—Cl1	102.65 (5)	N2—Hg1—O1	65.35 (6)
N1—Hg1—Cl1	101.29 (6)	N1—Hg1—O1	65.59 (7)
N2—Hg1—Cl2	101.97 (5)	Cl1—Hg1—O1	133.20 (4)
N1—Hg1—Cl2	103.41 (6)	Cl2—Hg1—O1	106.62 (4)

Table 2
Overview of pyridyl–pyridyl ring geometry metrics (Å, °) for [Hg**L**Cl_2] (**1**).

*Cg*1 and *Cg*2 are the centroids of the N1/C1–C5 and N2/C8–C12 rings, respectively.

Centroids	Dihedral angle between rings	Centroid–centroid distance	Centroid–plane distance	Centroid offset
$Cg1\cdots Cg1^{i}$	0.00	3.718 (2)	3.573 (2)	1.028
$Cg2\cdots Cg2^{ii}$	0.00	4.002 (2)	3.563 (4)	1.822
$Cg2\cdots Cg2^{iii}$	0.00	5.005 (2)	3.536 (4)	3.542
$Cg1\cdots Cg2^{iii}$	18.38 (12)	4.2944 (15)	2.826 (4)	3.233
$Cg2\cdots Cg1^{iii}$	18.38 (12)	4.2944 (15)	3.702 (3)	2.176

Symmetry codes: (i) $-x+1, -y+2, -z+1$; (ii) $-x, -y+1, -z+1$; (iii) $-x+1, -y+1, -z+1$.

2. Structural commentary

Complex **1** crystallizes in the monoclinic space group $P2_1/n$ as a monomer (Fig. 1). The tridentate ligand and two chlorides provide a slightly distorted square-pyramidal geometry (τ = 0.07; Table 1) to the metal ion (Addison *et al.* 1984). In the complex, tridentate **L** has an asymmetrical, slightly bent conformation in the basal plane with an N1—Hg1—N2 angle of 129.28 (8)°. Both chelate rings have an envelope conformation with O1 in the flap position. The mercury atom is 0.8100 (9) Å above the basal plane. The apical Hg—Cl distance is 0.0083 Å longer than the basal Hg—Cl distance.

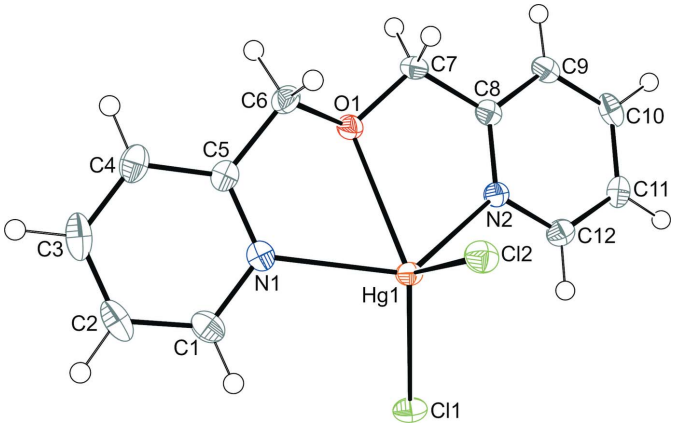

Figure 1
The molecular structure of **1** with the atom-numbering scheme generated with *ORTEP-3 for Windows* (Farrugia, 2012). Displacement ellipsoids are drawn at the 50% probability level and H atoms are displayed as small spheres of arbitrary radii.

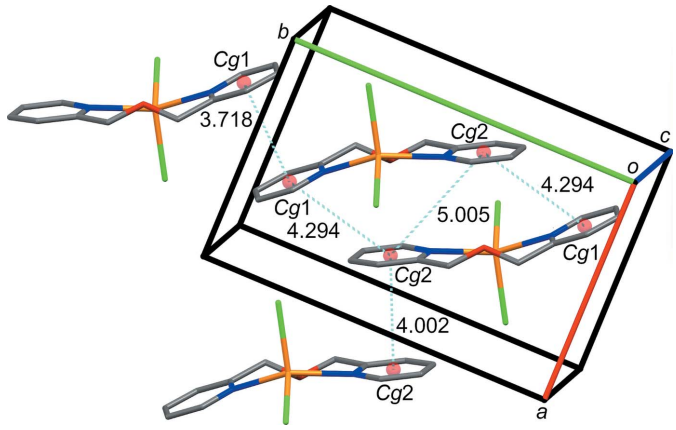

Figure 2
Offset face-to-face pyridyl ring arrangement between inversion-related molecules of **1** illustrated using *Mercury 2020.1* (Macrae *et al.*, 2020). Ring centroids are shown as red spheres. Blue dashed lines show centroid–centroid distances (for numerical data, see Table 2).

3. Supramolecular features

The packing of **1** is stabilized by π–π stacking interactions (Fig. 2) and van der Waals interactions (Fig. 3). On the apical side of **1**, pyridyl rings (centroids *Cg*1: N1/C1–C5; *Cg*2: N2/C8–C12) are stacked against separate inversion-related equivalents with a small offset (Table 2). In contrast, the basal face features an extended ligand conformation placing the N2 pyridyl rings across from the chelate rings of an inversion-related molecule (Fig. 2) with large offsets between the pyridyl ring centroids of the opposing ligand (Table 2). Although the large centroid offsets preclude π–π stacking interactions on the basal face, the predominantly planar ligand allows the inner and outer edges of N2 pyridyl rings to nestle along the inner edges of opposing N2 and N1 pyridyl rings, respectively (Fig. 2).

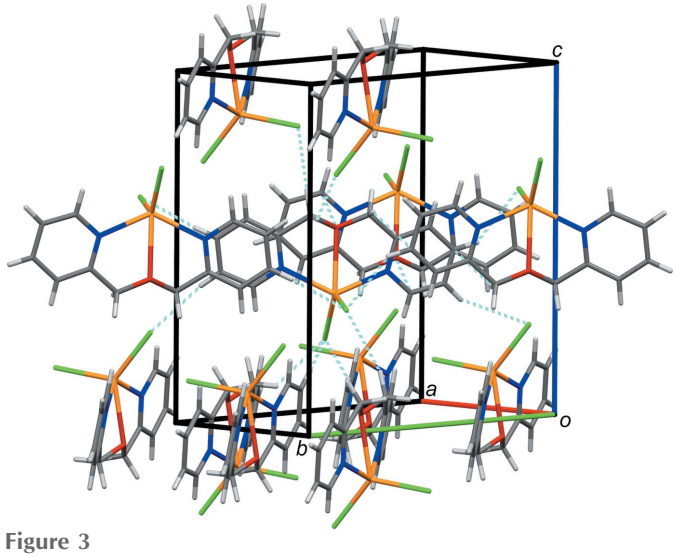

Figure 3
Crystal packing of compound **1** illustrated using *Mercury* 2020.1 (Macrae *et al.*, 2020). Face-to-face aromatic interactions occur within sheets of molecules in the *ab* plane. Short interatomic contacts within and between the sheets of **1** are shown by blue dashed lines (for numerical data, see Table 4).

Table 3
Hydrogen-bond geometry (Å, °).

D—H···A	D—H	H···A	D···A	D—H···A
C2—H2···Cl1^{i}	0.95	2.73	3.623 (3)	157
C6—H6B···Cl2^{ii}	0.99	2.79	3.746 (3)	164
C6—H6A···Cl1^{iii}	0.99	2.94	3.711 (3)	135
C11—H11···Cl1^{iv}	0.95	2.86	3.722 (3)	151

Symmetry codes: (i) $-x+\frac{3}{2}, y+\frac{1}{2}, -z+\frac{1}{2}$; (ii) $x+\frac{1}{2}, -y+\frac{3}{2}, z+\frac{1}{2}$; (iii) $x-\frac{1}{2}, -y+\frac{3}{2}, z+\frac{1}{2}$; (iv) $-x+\frac{1}{2}, y-\frac{1}{2}, -z+\frac{1}{2}$.

Aromatic stacking interactions contribute to formation of sheets parallel to the *ab* plane. Adjacent sheets are related by a 2_1 screw axis. Intermolecular van der Waals interactions, some of which could be described as weak hydrogen bonds involving C—H donors and Cl acceptors (Table 3; Brammer *et al.*, 2001), occur within and between the sheets.

4. Hirshfeld surface analysis

Intermolecular interactions were investigated by quantitative analysis of the Hirshfeld surface and visualized with *CrystalExplorer 21.5* (Spackman *et al.*, 2021). Five hourglass features appeared on the Hirshfeld surface of **1** plotted over shape index (Fig. 4). Both hourglass features on the apical side reflect self-complementary face-to-face bump and hollow alignments between inversion-related pyridyl rings involved in π–π stacking. The hourglass features associated with O1 and C12 on the basal face arise from the bend of the O atom in the flap position of the chelate rings towards the inversion-related molecule (Fig. 2), resulting in notably shorter interatomic

Table 4
Short interatomic contacts (Å) in [Hg**L**Cl$_2$] (**1**).

Atoms	Distance	Atoms	Distance
Cl1···H2^{i}	2.732	Cl2···H6B^{ii}	2.785
Cl2···H3^{iii}	2.808	Cl2···H10^{iv}	2.813
H11···Cl1^{v}	2.862	O1···C12^{vi}	3.201 (3)

Symmetry codes: (i) $-x+\frac{3}{2}, y-\frac{1}{2}, -z+\frac{1}{2}$; (ii) $x-\frac{1}{2}, -y+\frac{3}{2}, z-\frac{1}{2}$; (iii) $-x+1, -y+2, -z+1$; (iv) $-x, -y+1, -z+1$; (v) $-x+\frac{1}{2}, y-\frac{1}{2}, -z+\frac{1}{2}$; (vi) $-x+1, -y+1, -z+1$.

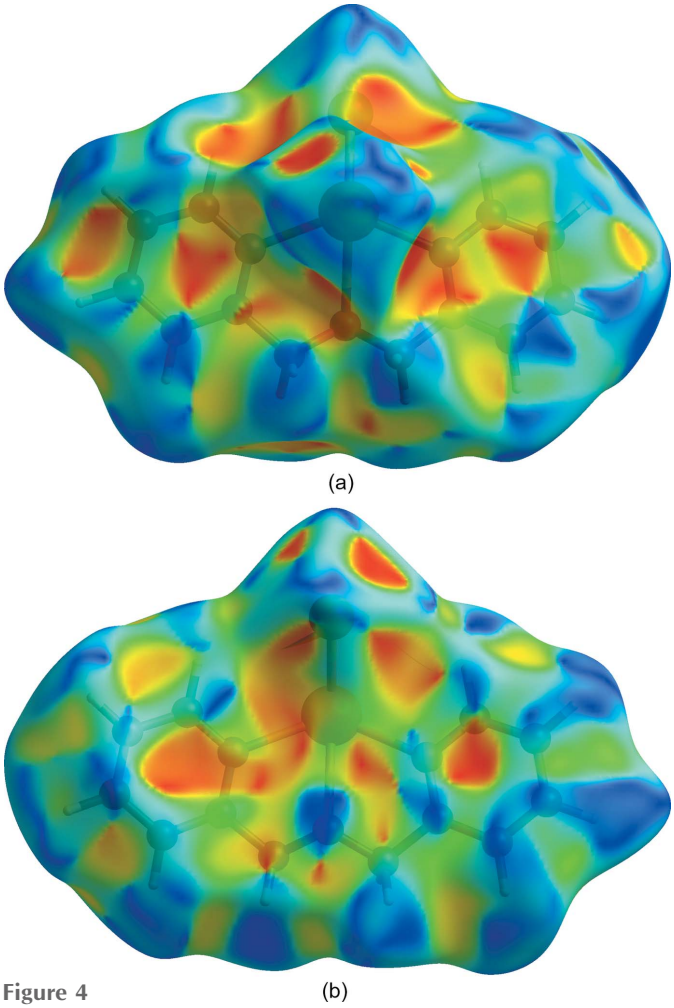

Figure 4
(*a*) Apical and (*b*) basal plane views of the Hirshfeld surface of **1** plotted over shape index generated with *CrystalExplorer* 21.5 (Spackman *et al.* 2021). Blue and red areas represent bumps and hollow regions, respectively, on the shape-index surface.

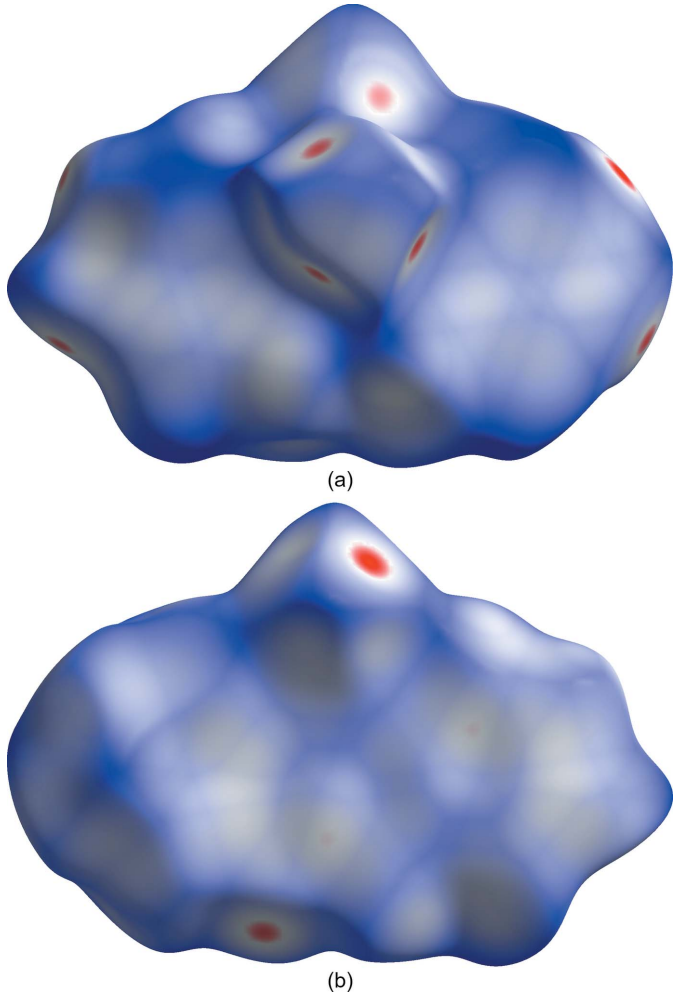

Figure 5
Views of the (*a*) apical and (*b*) basal plane Hirshfeld surface of **1** plotted over normalized contact distance (d_{norm}) in the range from −0.1617 to 1.4660 a.u. generated with *CrystalExplorer* 21.5 (Spackman *et al.* 2021). Intermolecular contacts closer than the sum of their van der Waals radii are highlighted in red on the d_{norm} surface. Contacts near and longer than the sum of van der Waals radii are shown in white and blue, respectively.

distances than for adjacent atoms (Table 4). The last hourglass feature reflects surface complementarity near the interior edges of inversion-related N2 pyridyl rings with a centroid offset of 3.452 Å. Additional blue and red horseshoe-shaped regions on the basal face correlate with a bump along the C9—C10 outer edge of the N2 pyridyl ring nesting against a hollow looping around N1, respectively.

The Hirshfeld surface of **1** mapped with the function d_{norm}, the sum of the distances from a surface point to the nearest interior (d_i) and exterior (d_e) atoms normalized by the van der Waals (vdW) radii of the corresponding atom (r_{vdW}), is shown in Fig. 5. Contacts shorter than the sums of vdW radii are shown in red, those longer in blue, and those approximately equal as white spots. The most intense red spots correspond to a series of intermolecular contacts between the peripheral chlorine atoms and hydrogen atoms with Cl···H distances of 2.7319–2.8616 Å (Table 4), some of which could be regarded as weak hydrogen bonds (Brammer *et al.* 2001). There are also very faint red spots on the basal planes associated with an O1···C12 contact.

The overall 2D fingerprint plot for **1** is provided in Fig. 6*a*. Interactions delineated into Cl···H/H···Cl (36.5%), H···H (36.5%) and H···Cl/H···Cl (11.6%) contacts are shown in Fig. 6*b–d*. Other minor contributions to the Hirshfeld surface are from C···C (4.1%), N···H/H···N (3.1%), O···C/C···O (2.8%), N···C/C···N (2.7%), Hg···C/C···Hg (0.7%), Hg···H/H···Hg (0.7%), O···N/N···O (0.7%), and Cl···C/C···Cl (0.5%) interactions.

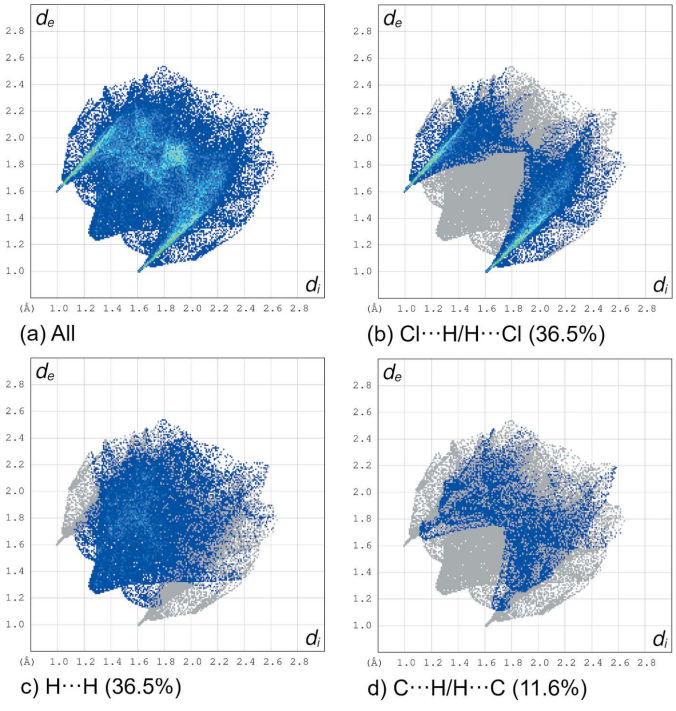

Figure 6
The full two-dimensional fingerprint plots for **1**, showing (*a*) all interactions, and components delineated into (*b*) Cl···H/H···Cl, (*c*) H···H, and (*d*) C···H/H···C interactions generated with *CrystalExplorer* 21.5 (Spackman *et al.* 2021). The d_i and d_e values are closest internal and external distances (in Å) from given points on the Hirshfeld surface.

5. Database survey

A search of the Cambridge Structural Database (CSD, Version 5.43, update of June 2022; Groom *et al.*, 2016) for complexes of mercury bound to an ether oxygen, two nitrogen and two chloride atoms yielded seven hits. Unlike the bis-aliphatic ether component of **1**, all reported structures involved derivatized anisole ligands.

A search of the Cambridge Structural Database (CSD, Version 5.43, update of June 2022; Groom *et al.*, 2016) for **L** yielded fourteen hits. Four [*M***L**Cl_2] complexes isotypic with **1** have been reported with *M* = Co (refcode RAVMOU; Misawa-Suzuki *et al.*, 2022), Cu (refcode UGANIA; Li, 2008*a*), Zn (refcode UGANOG; Li, 2008*b*) and Cd (refcode TIGJID; Li, 2007). The isotypic complexes have square-pyramidal coordination geometries (τ = 0.03–0.14) and extended ligand conformations with slightly smaller pyridyl ring dihedral angles (range 12.88–16.85°) compared to **1**. An extended conformation of **L** has also been reported in meridional octahedral complexes [Cr**L**Cl_3]·H_2O (refcode ZAXBUX; Chen *et al.*, 2012), [Fe**L**Cl_3] (refcode RAVXEV; Misawa-Suzuki *et al.*, 2022), [Co$\mathbf{L}_2$]$(PF_6)_2$ (refcode RAVLAF; Misawa-Suzuki *et al.*, 2022), [Cd$\mathbf{L}_2$]$(ClO_4)_2$·CH_3CN (refcode VAXXOL; Sturner *et al.*, 2022), and [Zn$\mathbf{L}_2$]$(ClO_4)_2$·CH_3CN (refcode VAYCEH; Sturner *et al.*, 2022), as well as the discrete square-planar and square-pyramidal cations of [Cu**L**Cl]-[Cu**L**Cl(H_2O)]$(ClO_4)_2$ (refcode FOWJAD: Li *et al.*, 2009). In contrast, substantially bent conformations of **L** are observed in slightly distorted octahedral facial complexes [Rh**L**Cl_3]·-CH_2Cl_2 (refcode AWOQIN; Ojwach *et al.*, 2011), [Mo**L**$(CO)_3$] (refcode GUGWAG; Nanty *et al.*, 2000) and (2,2′-bipyridine)(2,2′-[oxybis(methylidene)]dipyridine)(perchlorato)-copper(II) perchlorate (refcode IXUYEF; Cheng *et al.*, 2004) and distorted trigonal–prismatic [Hg$\mathbf{L}_2$]$(ClO_4)_2$ (refcode VAXXUR; Sturner *et al.*, 2022). The published structures document the coordinative flexibility of **L**.

6. Synthesis and crystallization

A solution of **L** (41 mg, 205 µmol) in 3 mL methanol was added to one equivalent of $HgCl_2$ (55 mg, 203 µmol) in 12 mL of methanol with stirring. The resulting precipitate was dissolved with the addition of 35 mL of methanol. The solution was filtered through Celite and fractionated. Pale-pink needles were obtained through slow evaporation (52 mg, 110 µmol, 54% yield), m.p.: 423–426 K. ^{1}H NMR (CD_3CN, nominally 2 m*M*, 293 K) δ: 8.69 (*d*, 2H, *J* = 5.4 Hz), 7.95 (*ddd*, 2H, *J* = 8.0, 8.0, 1.9 Hz), 7.53 (*m*, 2H), 4.88 (*s*, 4H). IR (ATR) ν/cm^{-1}: 3080(*w*), 3069(*w*), 3028(*w*), 2864(*w*), 1602(*s*), 1574(*m*), 1487(*m*), 1465(*m*), 1449(*s*), 1406(*m*), 1385(*w*), 1364(*m*), 1301(*m*), 1288(*s*), 1250(*m*), 1231(*w*), 1221(*m*), 1163(*m*), 1155(*m*), 1130(*s*), 1109(*m*), 1099(*s*), 1051(*m*), 1030(*m*), 1016(*s*), 1003(*m*), 995(*m*), 972(*w*), 961(*w*), 889(*w*), 851(*m*), 826(*w*), 816(*w*), 810(*w*), 773(*s*), 762(*s*), 723(*s*), 667(*w*), 646(*m*), 640(*s*), 629(*m*). Elemental analysis calculated for $C_{12}H_{12}HgN_2O$: C, 30.55; H, 2.56; N, 5.94. Found: C, 30.54; H, 2.51; N, 5.90%.

Table 5
Experimental details.

Crystal data	
Chemical formula	$[HgCl_2(C_{12}H_{12}N_2O)]$
M_r	471.73
Crystal system, space group	Monoclinic, $P2_1/n$
Temperature (K)	100
a, b, c (Å)	8.0202 (6), 12.587 (1), 13.7761 (11)
β (°)	91.290 (1)
V (Å^3)	1390.35 (19)
Z	4
Radiation type	Mo $K\alpha$
μ (mm^{-1})	11.44
Crystal size (mm)	0.46 × 0.16 × 0.14
Data collection	
Diffractometer	Bruker *SMART* APEXII CCD
Absorption correction	Numerical (*SADABS*; Krause *et al.*, 2015)
T_{min}, T_{max}	0.144, 0.486
No. of measured, independent and observed [$I > 2\sigma(I)$] reflections	20815, 2763, 2638
R_{int}	0.022
(sin $\theta/\lambda)_{max}$ (Å^{-1})	0.619
Refinement	
$R[F^2 > 2\sigma(F^2)]$, $wR(F^2)$, S	0.014, 0.034, 1.09
No. of reflections	2763
No. of parameters	163
H-atom treatment	H-atom parameters constrained
$\Delta\rho_{max}$, $\Delta\rho_{min}$ (e Å^{-3})	0.87, −0.32

Computer programs: *APEX3* (Bruker, 2015), *SAINT-Plus* (Bruker, 2012), *SHELXS2014/5* (Sheldrick, 2015*a*), *SHELXL2014/5* (Sheldrick, 2015*b*), *ShelXle* (Hübschle, 2011), *ORTEP-3 for Windows* (Farrugia, 2012), *Mercury* (Macrae *et al.*, 2020), *CrystalExplorer21.5* (Spackman *et al.*, 2021), *OLEX2* (Dolomanov *et al.*, 2009), and *publCIF* (Westrip, 2010).

7. Refinement

Crystal data, data collection and structure refinement details are summarized in Table 5. The hydrogen atoms were placed in calculated positions with C—H distances of 0.95 Å (aromatic) and 0.99 Å (methylene) and refined as riding atoms with $U_{iso}(H) = 1.2U_{eq}(C)$.

Acknowledgements

The authors thank Professor Robert Pike for consulting on this work and for the extraordinary patience he has demonstrated while providing training in X-ray crystallography over the past seventeen years.

Funding information

Funding for this research was provided by: William & Mary; National Science Foundation, Directorate for Mathematical and Physical Sciences (grant No. 0443345).

References

Addison, A. W., Rao, T. N., Reedijk, J., van Rijn, J. & Verschoor, G. C. (1984). *J. Chem. Soc. Dalton Trans.* pp. 1349–1356.

Brammer, L., Bruton, E. A. & Sherwood, P. (2001). *Cryst. Growth Des.* **1**, 277–290.

Bruker (2012). *SAINT-Plus*. Bruker AXS Inc. Madison, Wisconsin, USA.

Bruker (2015). *APEX3*. Bruker AXS Inc. Madison, Wisconsin, USA.

Chen, F., Lu, X., Chen, X., Li, H. & Hu, Y. (2012). *Inorg. Chim. Acta*, **387**, 407–411.

Cheng, Y., Chen, H., Tsai, S., Su, C., Tsang, H., Kuo, T., Tsai, Y., Liao, F. & Wang, S. (2004). *Eur. J. Inorg. Chem.* pp. 2180–2188.

Dolomanov, O. V., Bourhis, L. J., Gildea, R. J., Howard, J. A. K. & Puschmann, H. (2009). *J. Appl. Cryst.* **42**, 339–341.

Farrugia, L. J. (2012). *J. Appl. Cryst.* **45**, 849–854.

Groom, C. R., Bruno, I. J., Lightfoot, M. P. & Ward, S. C. (2016). *Acta Cryst.* B**72**, 171–179.

Hübschle, C. B., Sheldrick, G. M. & Dittrich, B. (2011). *J. Appl. Cryst.* **44**, 1281–1284.

Ivanova, J., Pantcheva, I. N., Mitewa, M., Simova, S., Tanabe, M. & Osakada, K. (2011). *Chem. Cent. J.* **5**, 52.

Kim, E., Pai, T. & Han, O. (2011). *J. Agric. Food Chem.* **59**, 3606–3612.

Krause, L., Herbst-Irmer, R., Sheldrick, G. M. & Stalke, D. (2015). *J. Appl. Cryst.* **48**, 3–10.

Li, H., Xie, L. M. & Zhang, S. G. (2009). *Acta Cryst.* E**65**, m933.

Li, J. M. (2007). *Acta Cryst.* E**63**, m2241.

Li, J. M. (2008*a*). *Acta Cryst.* E**64**, m1467.

Li, J. M. (2008*b*). *Acta Cryst.* E**64**, m1468.

Li, X., Jiang, X., Sun, J., Zhu, C., Li, X., Tian, L., Liu, L. & Bai, W. (2017). *Ann. N. Y. Acad. Sci.* **1398**, 5–19.

Macrae, C. F., Sovago, I., Cottrell, S. J., Galek, P. T. A., McCabe, P., Pidcock, E., Platings, M., Shields, G. P., Stevens, J. S., Towler, M. & Wood, P. A. (2020). *J. Appl. Cryst.* **53**, 226–235.

Misawa-Suzuki, T., Ikeda, R., Komatsu, R., Toriba, R., Miyamoto, R. & Nagao, H. (2022). *Polyhedron*, **218**, 115735.

Nanty, D., Laurent, M., Khan, M. A. & Ashby, M. T. (2000). *Acta Cryst.* C**56**, 35–36.

Ojwach, S. O., Omondi, B. & Darkwa, J. (2011). *Acta Cryst.* E**67**, m1097.

Sheldrick, G. M. (2015*a*). *Acta Cryst.* A**71**, 3–8.

Sheldrick, G. M. (2015*b*). *Acta Cryst.* C**71**, 3–8.

Spackman, P. R., Turner, M. J., McKinnon, J. J., Wolff, S. K., Grimwood, D. J., Jayatilaka, D. & Spackman, M. A. (2021). *J. Appl. Cryst.* **54**, 1006–1011.

Sreenivasulu, K., Raghu, P. & Nair, K. M. (2010). *J. Food Sci.* **75**, H123–H128.

Sturner, M. A., Starr, I. J., Owusu-Koramoah, J. E., Brewster, A. D., Pike, R. D. & Bebout, D. C. (2022). *Polyhedron*, **217**, 115727.

Westrip, S. P. (2010). *J. Appl. Cryst.* **43**, 920–925.

Zhang, W., Zhi, J., Cui, Y., Zhang, F., Habyarimana, A., Cambier, C. & Gustin, P. (2014). *PLoS One*, **9**, e109136.

supporting information

Acta Cryst. (2022). E**78**, 1233-1237 [https://doi.org/10.1107/S2056989022010878]

Crystal structure and Hirshfeld surface analysis of dichlorido{2,2′-[oxybis(methylidene)]dipyridine}mercury(II)

Jesse J. Derringer and Deborah C. Bebout

Computing details

Data collection: *APEX3* (Bruker, 2015); cell refinement: *SAINT-Plus* (Bruker, 2012); data reduction: *SAINT-Plus* (Bruker, 2012); program(s) used to solve structure: *SHELXS2014/5* (Sheldrick, 2015a); program(s) used to refine structure: *SHELXL2014/5* (Sheldrick, 2015b); molecular graphics: *ShelXle* (Hübschle, 2011); software used to prepare material for publication: *ORTEP-3 for Windows* (Farrugia, 2012), *Mercury* (Macrae *et al.*, 2020), CrystalExplorer 21.5 (Spackman *et al.*, 2021), OLEX2 (Dolomanov *et al.*, 2009), and *publCIF* (Westrip, 2010).

Dichlorido{2,2′-[oxybis(methylidene)]dipyridine}mercury(II)

Crystal data

$[HgCl_2(C_{12}H_{12}N_2O)]$
M_r = 471.73
Monoclinic, $P2_1/n$
a = 8.0202 (6) Å
b = 12.587 (1) Å
c = 13.7761 (11) Å
β = 91.290 (1)°
V = 1390.35 (19) Å^3
Z = 4
$F(000)$ = 880
D_x = 2.254 Mg m^{-3}
Mo $K\alpha$ radiation, λ = 0.71073 Å
Cell parameters from 9936 reflections
θ = 2.9–26.1°
μ = 11.44 mm^{-1}
T = 100 K
Needle, pink
0.46 × 0.16 × 0.14 mm

Data collection

Bruker SMART APEXII CCD diffractometer
Radiation source: fine-focus sealed tube
Graphite monochromator
ω and ψ scans
Absorption correction: numerical (SADABS; Krause *et al.*, 2015)
T_{min} = 0.144, T_{max} = 0.486
20815 measured reflections
2763 independent reflections
2638 reflections with $I > 2\sigma(I)$
R_{int} = 0.022
θ_{max} = 26.1°, θ_{min} = 2.2°
h = −9→9
k = −15→15
l = −17→17

Refinement

Refinement on F^2
Least-squares matrix: full
$R[F^2 > 2\sigma(F^2)]$ = 0.014
$wR(F^2)$ = 0.034
S = 1.09
2763 reflections
163 parameters
0 restraints
Primary atom site location: other
Hydrogen site location: inferred from neighbouring sites
H-atom parameters constrained
$w = 1/[\sigma^2(F_o^2) + (0.0174P)^2 + 1.5258P]$ where $P = (F_o^2 + 2F_c^2)/3$
$(\Delta/\sigma)_{max}$ = 0.001
$\Delta\rho_{max}$ = 0.87 e Å^{-3}
$\Delta\rho_{min}$ = −0.32 e Å^{-3}

Special details

Geometry. All esds (except the esd in the dihedral angle between two l.s. planes) are estimated using the full covariance matrix. The cell esds are taken into account individually in the estimation of esds in distances, angles and torsion angles; correlations between esds in cell parameters are only used when they are defined by crystal symmetry. An approximate (isotropic) treatment of cell esds is used for estimating esds involving l.s. planes.

Fractional atomic coordinates and isotropic or equivalent isotropic displacement parameters (Å²)

	x	*y*	*z*	U_{iso}*/U_{eq}
Hg1	0.38378 (2)	0.68896 (2)	0.36993 (2)	0.01728 (4)
Cl1	0.55569 (8)	0.63592 (5)	0.23324 (5)	0.02356 (14)
Cl2	0.12028 (8)	0.78490 (5)	0.34042 (5)	0.02342 (14)
O1	0.4165 (2)	0.66608 (14)	0.55572 (13)	0.0180 (4)
N1	0.5538 (3)	0.81512 (16)	0.44555 (17)	0.0188 (5)
N2	0.2909 (3)	0.52695 (17)	0.42871 (15)	0.0165 (4)
C1	0.6644 (3)	0.8701 (2)	0.3933 (2)	0.0244 (6)
H1	0.672585	0.855181	0.326020	0.029*
C2	0.7663 (3)	0.9472 (2)	0.4339 (2)	0.0294 (7)
H2	0.842884	0.985000	0.395143	0.035*
C3	0.7549 (4)	0.9686 (2)	0.5324 (2)	0.0309 (7)
H3	0.821863	1.022269	0.562062	0.037*
C4	0.6442 (3)	0.9103 (2)	0.5865 (2)	0.0257 (6)
H4	0.636434	0.922285	0.654331	0.031*
C5	0.5445 (3)	0.8344 (2)	0.54108 (19)	0.0182 (5)
C6	0.4211 (3)	0.7698 (2)	0.59698 (19)	0.0211 (5)
H6B	0.455937	0.765959	0.666302	0.025*
H6A	0.309279	0.802897	0.592423	0.025*
C7	0.2934 (3)	0.5986 (2)	0.59428 (18)	0.0197 (5)
H7A	0.191536	0.639976	0.607620	0.024*
H7B	0.334940	0.567189	0.656137	0.024*
C8	0.2531 (3)	0.5114 (2)	0.52223 (18)	0.0173 (5)
C9	0.1749 (3)	0.4187 (2)	0.55252 (19)	0.0203 (5)
H9	0.151175	0.408214	0.619088	0.024*
C10	0.1324 (3)	0.3420 (2)	0.4844 (2)	0.0229 (6)
H10	0.075338	0.279417	0.503154	0.027*
C11	0.1740 (3)	0.3577 (2)	0.3883 (2)	0.0215 (6)
H11	0.148269	0.305511	0.340459	0.026*
C12	0.2539 (3)	0.4508 (2)	0.36382 (19)	0.0204 (5)
H12	0.283764	0.461234	0.298171	0.024*

Atomic displacement parameters (Å²)

	U^{11}	U^{22}	U^{33}	U^{12}	U^{13}	U^{23}
Hg1	0.01956 (6)	0.01822 (6)	0.01414 (6)	−0.00100 (4)	0.00190 (4)	0.00056 (3)
Cl1	0.0263 (3)	0.0269 (3)	0.0177 (3)	0.0048 (3)	0.0053 (3)	0.0001 (3)
Cl2	0.0203 (3)	0.0259 (3)	0.0241 (3)	0.0031 (3)	0.0017 (3)	0.0013 (3)
O1	0.0181 (9)	0.0178 (9)	0.0181 (9)	−0.0010 (7)	0.0033 (7)	−0.0015 (7)
N1	0.0179 (11)	0.0155 (11)	0.0229 (12)	0.0018 (8)	0.0003 (9)	0.0010 (8)

N2	0.0146 (10)	0.0185 (11)	0.0165 (10)	0.0019 (8)	−0.0002 (8)	0.0004 (8)
C1	0.0230 (14)	0.0212 (13)	0.0291 (15)	0.0012 (11)	0.0045 (11)	0.0046 (11)
C2	0.0193 (14)	0.0205 (14)	0.0485 (19)	−0.0029 (11)	0.0022 (13)	0.0095 (13)
C3	0.0234 (15)	0.0177 (14)	0.051 (2)	−0.0022 (11)	−0.0094 (14)	−0.0026 (13)
C4	0.0249 (14)	0.0213 (14)	0.0306 (15)	0.0027 (11)	−0.0059 (12)	−0.0049 (11)
C5	0.0176 (13)	0.0155 (12)	0.0212 (13)	0.0045 (10)	−0.0024 (11)	−0.0011 (10)
C6	0.0226 (14)	0.0216 (13)	0.0191 (13)	0.0004 (11)	0.0013 (11)	−0.0054 (11)
C7	0.0200 (13)	0.0233 (13)	0.0158 (12)	−0.0017 (10)	0.0036 (10)	0.0017 (10)
C8	0.0130 (12)	0.0201 (13)	0.0189 (13)	0.0036 (10)	−0.0005 (10)	0.0034 (10)
C9	0.0162 (12)	0.0231 (13)	0.0216 (13)	0.0023 (10)	0.0010 (10)	0.0064 (11)
C10	0.0148 (13)	0.0179 (13)	0.0360 (16)	−0.0006 (10)	−0.0011 (11)	0.0065 (11)
C11	0.0183 (13)	0.0195 (13)	0.0264 (14)	−0.0002 (11)	−0.0041 (11)	−0.0036 (11)
C12	0.0209 (13)	0.0211 (13)	0.0191 (13)	0.0032 (11)	−0.0010 (10)	0.0009 (10)

Geometric parameters (Å, º)

Hg1—N2	2.323 (2)	C4—C5	1.386 (4)
Hg1—N1	2.324 (2)	C4—H4	0.9500
Hg1—Cl1	2.4515 (6)	C5—C6	1.506 (4)
Hg1—Cl2	2.4598 (7)	C6—H6B	0.9900
Hg1—O1	2.5831 (18)	C6—H6A	0.9900
O1—C7	1.415 (3)	C7—C8	1.510 (4)
O1—C6	1.424 (3)	C7—H7A	0.9900
N1—C5	1.342 (4)	C7—H7B	0.9900
N1—C1	1.346 (4)	C8—C9	1.393 (4)
N2—C12	1.340 (3)	C9—C10	1.384 (4)
N2—C8	1.344 (3)	C9—H9	0.9500
C1—C2	1.379 (4)	C10—C11	1.386 (4)
C1—H1	0.9500	C10—H10	0.9500
C2—C3	1.389 (5)	C11—C12	1.381 (4)
C2—H2	0.9500	C11—H11	0.9500
C3—C4	1.382 (4)	C12—H12	0.9500
C3—H3	0.9500		

N2—Hg1—N1	129.28 (8)	N1—C5—C4	121.5 (3)
N2—Hg1—Cl1	102.65 (5)	N1—C5—C6	117.1 (2)
N1—Hg1—Cl1	101.29 (6)	C4—C5—C6	121.4 (2)
N2—Hg1—Cl2	101.97 (5)	O1—C6—C5	107.6 (2)
N1—Hg1—Cl2	103.41 (6)	O1—C6—H6B	110.2
Cl1—Hg1—Cl2	120.18 (2)	C5—C6—H6B	110.2
N2—Hg1—O1	65.35 (6)	O1—C6—H6A	110.2
N1—Hg1—O1	65.59 (7)	C5—C6—H6A	110.2
Cl1—Hg1—O1	133.20 (4)	H6B—C6—H6A	108.5
Cl2—Hg1—O1	106.62 (4)	O1—C7—C8	109.3 (2)
C7—O1—C6	114.40 (19)	O1—C7—H7A	109.8
C7—O1—Hg1	112.52 (14)	C8—C7—H7A	109.8
C6—O1—Hg1	107.13 (14)	O1—C7—H7B	109.8
C5—N1—C1	118.9 (2)	C8—C7—H7B	109.8

C5—N1—Hg1	121.20 (18)	H7A—C7—H7B	108.3
C1—N1—Hg1	119.92 (19)	N2—C8—C9	121.4 (2)
C12—N2—C8	118.9 (2)	N2—C8—C7	118.3 (2)
C12—N2—Hg1	117.63 (17)	C9—C8—C7	120.2 (2)
C8—N2—Hg1	122.88 (17)	C10—C9—C8	119.1 (2)
N1—C1—C2	122.5 (3)	C10—C9—H9	120.4
N1—C1—H1	118.7	C8—C9—H9	120.4
C2—C1—H1	118.7	C9—C10—C11	119.2 (2)
C1—C2—C3	118.7 (3)	C9—C10—H10	120.4
C1—C2—H2	120.6	C11—C10—H10	120.4
C3—C2—H2	120.6	C12—C11—C10	118.5 (2)
C4—C3—C2	118.8 (3)	C12—C11—H11	120.7
C4—C3—H3	120.6	C10—C11—H11	120.7
C2—C3—H3	120.6	N2—C12—C11	122.8 (2)
C3—C4—C5	119.5 (3)	N2—C12—H12	118.6
C3—C4—H4	120.2	C11—C12—H12	118.6
C5—C4—H4	120.2		

C5—N1—C1—C2	−1.4 (4)	C6—O1—C7—C8	157.7 (2)
Hg1—N1—C1—C2	178.8 (2)	Hg1—O1—C7—C8	35.2 (2)
N1—C1—C2—C3	0.3 (4)	C12—N2—C8—C9	−0.7 (4)
C1—C2—C3—C4	1.3 (4)	Hg1—N2—C8—C9	170.47 (18)
C2—C3—C4—C5	−1.7 (4)	C12—N2—C8—C7	−179.2 (2)
C1—N1—C5—C4	1.0 (4)	Hg1—N2—C8—C7	−8.0 (3)
Hg1—N1—C5—C4	−179.25 (19)	O1—C7—C8—N2	−20.4 (3)
C1—N1—C5—C6	−179.0 (2)	O1—C7—C8—C9	161.1 (2)
Hg1—N1—C5—C6	0.8 (3)	N2—C8—C9—C10	−1.3 (4)
C3—C4—C5—N1	0.6 (4)	C7—C8—C9—C10	177.1 (2)
C3—C4—C5—C6	−179.4 (3)	C8—C9—C10—C11	2.3 (4)
C7—O1—C6—C5	−174.0 (2)	C9—C10—C11—C12	−1.3 (4)
Hg1—O1—C6—C5	−48.6 (2)	C8—N2—C12—C11	1.8 (4)
N1—C5—C6—O1	35.2 (3)	Hg1—N2—C12—C11	−169.8 (2)
C4—C5—C6—O1	−144.8 (2)	C10—C11—C12—N2	−0.8 (4)

Hydrogen-bond geometry (Å, º)

D—H···*A*	*D*—H	H···*A*	*D*···*A*	*D*—H···*A*
C2—H2···Cl1^{i}	0.95	2.73	3.623 (3)	157
C6—H6*B*···Cl2^{ii}	0.99	2.79	3.746 (3)	164
C6—H6*A*···Cl1^{iii}	0.99	2.94	3.711 (3)	135
C11—H11···Cl1^{iv}	0.95	2.86	3.722 (3)	151

Symmetry codes: (i) −*x*+3/2, *y*+1/2, −*z*+1/2; (ii) *x*+1/2, −*y*+3/2, *z*+1/2; (iii) *x*−1/2, −*y*+3/2, *z*+1/2; (iv) −*x*+1/2, *y*−1/2, −*z*+1/2.